Comparison of imaging features of intrahepatic mass-forming cholangiocarcinoma on gadoxetic acid-enhanced MR imaging with and without chronic liver disease

Jae Min Kim

Department of Medicine

The Graduate School, Yonsei University

Comparison of imaging features of intrahepatic mass-forming cholangiocarcinoma on gadoxetic acid-enhanced MR imaging with and without chronic liver disease

Directed by Professor Myeong-Jin Kim

The Master's Thesis
submitted to the Department of Medicine
the Graduate School of Yonsei University
in partial fulfillment of the requirements for the degree
of Master of Medical Science

Jae Min Kim

June 2016

This certifies that the Master's Thesis of
Jae Min Kim is approved.

Thesis Supervisor : Myeong-Jin Kim

Thesis Committee Member#1 : Woo Jung Lee

Thesis Committee Member#2 : Do Young Kim

The Graduate School
Yonsei University

June 2016

ACKNOWLEDGEMENTS

First and foremost I express my gratitude to my supervisor, Professor Myeong-Jin Kim, who has sincerely guided and supported me throughout my thesis. Without his support, this work would not have been completed.

Furthermore I would like to thank Professor Jin-Young Choi, who led me onto the right path through the wise, precious advice steadily and patiently.

I am also extremely grateful to Professor Woo Jung Lee and Do Young Kim, for sparing me their valuable time to help complete this thesis.

I appreciate my family for everlasting trust and support, which deserve my sincere gratitude.

Finally, I must acknowledge my wife and best friend, Seon Young Hwang, without whose love and encouragement, I would not have finished this thesis.

<TABLE OF CONTENTS>

LIST OF FIGURES

LIST OF TABLES

ABSTRACT

Comparison of imaging features of intrahepatic mass-forming cholangiocarcinoma on gadoxetic acid-enhanced MR imaging with and without chronic liver disease

Jae Min Kim

Department of Medicine
The Graduate School, Yonsei University

(Directed by Professor Myeong-Jin Kim)

Objectives: To evaluate the differences in gadoxetic acid-enhanced MR imaging features of intrahepatic mass-forming cholangiocarcinomas (ICCs) between in patients with and without chronic liver disease (CLD).

Methods: Sixty-five patients (M:F=39:26, mean age, 63 [range, 35-80]) with ICCs who underwent preoperative gadoxetic acid-enhanced MRI retrospectively formed our study population. Among them, histopathology of the background liver revealed chronic hepatitis or liver cirrhosis in 20 patients, and no such diseases in 45 patients. Three observers independently reviewed imaging findings including (1) morphology; (2) pattern of enhancement; (3) appearance of T2-weighted image and diffusion weighted image. Statistically significant factors by univariable analyses (Chi-square test, Fisher's exact test or Mann-Whitney test) entered into multivariable analysis performed using logistic regression model.

Results: Univariable analyses revealed that peripheral location and proportion of arterial enhancement >20% of the tumor were significantly more frequent,

although peritumoral bile duct dilatation and diffuse bile duct dilatation were significantly less frequent in ICCs in CLD patients than those without CLD. On multivariable analysis, lack of peritumoral bile duct dilatation (P = .028, B = 1.721, odds ratio (OR) = 5.589) and proportion of arterial enhancement >20% (P = .028, B = 1.552, OR = 4.719) turned out to be the only independently significant differential feature.

Conclusion: ICCs arising in CLD patients more frequently show large area of arterial enhancement on gadoxetic acid-enhanced MR imaging and no peritumoral bile duct dilatation on T2-weighted MR image as compared to those developed in patients without CLD.

Key words : cholangiocarcinoma, diagnosis, chronic liver disease, magnetic resonance imaging, gadoxetic acid

Comparison of imaging features of intrahepatic mass-forming cholangiocarcinoma on gadoxetic acid-enhanced MR imaging with and without chronic liver disease

Jae Min Kim

Department of Medicine
The Graduate School, Yonsei University

(Directed by Professor Myeong-Jin Kim)

I. INTRODUCTION

Intrahepatic cholangiocarcinoma (ICC) is the second most common primary malignancy in the liver, next to hepatocellular carcinoma (HCC), arising from the epithelial cells of intrahepatic bile ducts [1]. Several studies revealed that the worldwide incidence of intrahepatic cholangiocarcinoma has been increased and long-term survival is poor [2-5]. Parasitic liver-flukes, primary sclerosing cholangitis, choledochal cysts, hepatolithiasis, and toxins are well known risk factors of ICC [6,7]. However, recent studies showed that cirrhosis, chronic hepatitis B or C, alcohol use, diabetes and obesity also increase the risk of ICC [8]. Specifically, chronic hepatitis or cirrhosis can induce mass-forming peripheral small duct type ICC [9]. Therefore, in patient with the chronic liver disease (CLD), it is important to distinguish the ICC especially mass forming type from HCC when the primary malignant tumor in the liver is suspected because ICC and HCC have significantly different management plans. The only curative treatment of ICC is surgical resection, whereas HCC can have various treatment plans including percutaneous ethanol injection, radiofrequency ablation and liver transplantation [4,10,11].

Magnetic resonance (MR) imaging is the commonly used for investigating focal hepatic lesion in clinical practice. Gadoxetic acid (Gd-EOB-DTPA ; Primovist® or Eovist®, Bayer Schering Pharma, Berlin, Germany) enables both dynamic and hepatobiliary phase (HBP) imaging for evaluation of focal liver lesions [12]. Gadoxetic acid-enhanced MRI can facilitate the detection of intrahepatic metastasis and conspicuity of ICC. Since the degree of enhancement of the liver parenchyma is affected by the liver function, the radiologic feature of ICC on gadoxetic acid-enhanced MRI may not be the same in normal liver and cirrhotic liver. Moreover ICC can be misdiagnosed as HCC on gadoxetic acid-enhanced MRI because gradual enhancement of the hepatic parenchyma may be interpreted as washout of HCC in cirrhotic liver. There have been no known studies regarding radiologic features of mass-forming ICC in the background liver of cirrhosis or chronic hepatitis on gadoxetic acid-enhanced MR imaging. Thus, the purpose of this study was to assess the distinguishable imaging features of mass-forming ICC of the CLD patients in comparison to normal background liver, using gadoxetic acid-enhanced MR imaging.

II. MATERIALS AND METHODS

1. Patient population

This retrospective study was approved by our institutional review board and was performed with waivers of informed consent. Patient confidentiality was guaranteed by using only anonymous data and radiological images. Our institutional database was searched for patients with pathologic diagnosis of ICC after surgical resection of liver and underwent preoperative liver MR imaging including gadoxetic acid-enhanced imaging between January 2008 and December 2013. The inclusion criteria were (1) pathologically proven ICCs by hepatic resection; (2) liver dynamic MR imaging performed in our institution

following standard protocol using gadoxetic acid as contrast material; and (3) no history of previous liver surgery, transcatheter arterial chemoembolization, percutaneous ethanol injection, or radiofrequency ablation before the imaging study.

2. MRI examinations

MRI was performed with a 3-T imaging system (MAGNETOM Tim Trio, Siemens Healthcare; Achieva, Philips Healthcare) equipped with a phased-array coil in our institution with standard protocol. The protocol consisted of a breath-hold transverse T1-weighted in- and out-of-phase 2D gradient-echo (GRE) sequence (TR/in phase TE, 150ms/2.4ms; out-of-phase TE, 1.2; flip angle, 65°; FOV, 32–38 × 25–29 cm; matrix, 256 × 256; section thickness, 6 mm; slice spacing, 1.2 mm; one signal acquired; number of slices, 30), a breath-hold transverse 3D GRE (TR/TE, 2.5/0.9; flip angle, 13°; FOV, 32–36 × 25–36 cm; matrix, 320 × 224; section thickness, 2 mm; no gap; acquisition time, 23 s) and a single shot turbo spin-echo (TR/TE, 466/148; FOV, 32–36 × 25–29 cm; matrix, 288 × 230; section thickness, 4 mm; gap, 1 mm) with spectral fat suppression technique. Parallel imaging with generalized auto-calibrating partially parallel acquisition with an acceleration factor of two was applied to improve image quality. Contrast-enhanced MRI was obtained using a breath-hold 3D GRE sequence after an IV bolus of 0.025 mmol/kg body weight of gadoxetic acid at an injection rate of 2 ml/s followed by a saline flush of 30 ml. Fluoroscopic bolus detection technique was used in all patients (Care-Bolus, Siemens Healthcare; BolusTrak, Philips Medical Systems) to determine the optimal timing for the hepatic arterial phase. The dynamic phases obtained after portal venous phase were collectively termed the transitional phase, and included the hepatic venous and late phase. Portal venous and transitional phase images were obtained approximately 30–40 s after the acquisition of the prior phase images; 20–35 s (arterial phase), 60–70 s (portal

venous phase), 100–180 s (transitional phase) after intravenous contrast injection. Hepatobiliary phase images were obtained 20 min after administration of contrast. An automatic infusion system (Sonic shot 50, NemotoKyorindo) was used. The actual pulse sequence was started manually when the fluoroscopic sequence revealed that the contrast material bolus had reached the abdominal aorta. Free-breathing diffusion weighted image (DWI) was also performed during the time interval between late phase imaging and hepatobiliary phase imaging using a single-shot, echo-planar sequence (3 directions of motion-probing gradients; b values of 50, 400, and 800 s/mm2; TR/TE, 1400/74; 2 number of excitations; matrix, 192 × 153; 8-mm slice thickness; acquisition time, 2-minute). The apparent diffusion coefficients (ADCs) were automatically calculated with the MR system for each diffusion weighted image and were presented as corresponding ADC maps.

3. Image analysis

All MR images are reviewed retrospectively by two abdominal radiologists (M.J.P. and Y.E.J., with 5 and 10 years' experiences of liver MRI) and one resident in radiology residency (J.M.K.) with knowledge of the pathologic diagnosis (ICCs). They independently evaluated pre-determined various MR features consisted of: A. location (center or periphery), margin, contour, and texture of the tumor, presence of central necrosis (fluid like T2-high SI, T1-low SI), presence of satellite nodule (additional lesion located ≤2cm from the tumor), multifocality (additional lesion located >2cm apart from the tumor), adjacent liver capsule retraction, bile duct dilatation (none, peritumoral or diffuse), hepatolithiasis, parenchymal atrophy, portal vein encasement/obliteration, portal vein thrombosis, hepatoduodenal lymphadenopathy (short axis diameter >1cm); (2) pattern of arterial enhancement (rim-like, global or mixed/irregular), proportion of arterial enhancement (≤ or >20% of the tumor area, >20% includes global, mixed and

thick rim like enhancement), dynamic enhancement pattern (progressive, stable or wash-out), peritumoral hyperemia, signal intensity on transitional phase, signal intensity on hepatobiliary phase, target appearance on hepatobiliary phase (central enhancement with hypointense rim), the presence of hyperintense rim on transitional phase; (3) hypointense rim on T2-weighted image, target appearance on high b-value diffusion-weighted image (b > 800 s/mm2, central hypointensity with peripheral hyperintense rim). Differences between the three observers were resolved by majority rule and consensus conference with another observer (J.Y.C. with 15 year's experiences of liver MRI).

As for multiple nodules, the largest lesion was analyzed and other lesions were classified as multifocality or satellite nodule. Observers did not aware of all other information such as patients' history, laboratory, and the background liver histology. The MR images of two groups were presented randomly. All images were reviewed using a Picture Archiving and Communication System (Centricity 3.0, General Electric Medical Systems, Milwaukee, WI).

4. Statistical analysis

The univariable statistical differences among each MRI parameter were analyzed using a Chi-square test or Fisher's exact test for categorical variables, and two-sample t-test for continuous variables. The statistically significant imaging features identified from univariable analysis entered into multivariable logistic regression analysis to reveal independent reliable findings of ICC in the patients with CLD compared to patients without liver cirrhosis or chronic hepatitis. Recurrence free survival data between two groups was evaluated via Kaplan-Meier curve and Log rank test. P-value of less than .05 was considered statistically significant. SPSS software package (version 20.0; Chicago, IL, USA) was used for statistical analyses. The inter-observer agreement for three observers was assessed by calculation of Fleiss-modified Kappa using the

freely available R software. The interpretation of Fleiss Kappa index for the strength of agreement followed the previous guidelines as poor (less than < 0); small (0.0–0.20); fair (0.21–0.40); moderate (0.41–0.60), substantial (0.61–0.80) and almost perfect (0.81–1.00) [13].

III. RESULTS

1. Baseline characteristics and pathologic findings

A total of 65 patients (39 men and 26 women; mean age, 63.0 years old) were included in our study according to the inclusion criteria. All histopathologic data of the patients following hepatic resection was reviewed, the background liver revealed CLD (chronic hepatitis or liver cirrhosis) in 20 patients (14 men and 26 women; mean age 63.2), and non-specific reactive liver histology in 45 patients (25 men and 20 women, mean age 62.9). Baseline characteristics and pathologic findings from surgical tumor specimen of the two groups (CLD and non-CLD group) are summarized in Table 1 and 2. The α-fetoprotein and aspartate aminotransferase (AST) level were significantly higher (P=0.026 and P=0.019, respectively) in CLD group.

Table 1. Baseline characteristics of all patients and comparison between patients with and without chronic liver disease (CLD).

	CLD patients with ICC (n=20)	Non-CLD patients with ICC (n=45)	P value*
Age (y)[a]	63.2 (40-79)	62.9 (36-80)	.926
Sex male/female	14 (70)/6 (30)	25 (55.6)/20 (44.4)	.273
Etiology of chronic liver disease			
Hepatitis B virus	9 (45)		
Hepatitis C virus	3 (15)		
Alcohol	5 (25)		
Unknown	3 (15)		
Chronic hepatitis/Cirrhosis (Child-Pugh A)	13 (65) /7 (35)		
Tumor marker			
AFP > 20 ng/ml	3 (15)	0 (0)	.026†
CEA > 5 μg/l	6 (30)	18 (40)	.441
CA19-9 > 37 U/ml	12 (60)	28 (62.2)	.865
Total bilirubin[b]	0.750 (0.3-4.5)	0.60 (0.2-4.2)	.096
AST[b]	32 (18-162)	24 (12-192)	.019†
ALT[b]	31.5 (8-82)	23 (6-268)	.499
Tumor diameter (cm) [a]	4.1 (1.2-9.3)	4.5 (1.4-8.6)	.387

Note: Unless otherwise specified, values are numbers of patients and numbers in parentheses are percentages. ICC, intrahepatic mass-forming cholangiocarcinoma; AFP, alphafetoprotein; CEA, carcinoembryonic antigen; CA19-9, carbohydrate antigen 19-9.

a Mean value with range in parentheses.

b Median value with range in parentheses.

*Chi-square test, Fisher's exact test, or two sample t-test.

†Statistically significant.

Table 2. Pathologic findings of the tumor from surgical resection in patients with and without chronic liver disease (CLD).

	CLD patients with ICC (n=20)	Non-CLD patients with ICC (n=45)	P value*
Tumor differentiation			.546
Well	4 (21.1)	8 (18.6)	
Moderate	11 (57.9)	30 (69.8)	
Poor	4 (21.1)	4 (9.3)	
Undifferentiated	0 (0)	1 (2.3)	
Resection margin			.117
Clear (R0)	17 (89.5)	31 (68.9)	
Not clear (R1)	2 (10.5)	14 (31.1)	
Microvessel invasion			.971
Not present	6 (31.6)	14 (31.1)	
Present	13 (68.4)	31 (68.9)	
Perineural invasion			.145
Not present	10 (71.4)	18 (48.6)	
Present	4 (28.6)	19 (51.4)	
Intrahepatic metastasis			.235
Not present	15 (78.9)	39 (90.7)	
Present	4 (21.1)	4 (9.3)	

Note: Values are numbers of patients and numbers in parentheses are percentages. ICC, intrahepatic mass-forming cholangiocarcinoma

Minor portion of the pathologic finding was omitted due to limited pathologic report data in retrospective review.

*Chi-square test or Fisher's exact test

2. Univariable and multivariable analyses results of MR imaging features

The MRI features of ICC in CLD patients group and non-CLD patients group are summarized in Appendices Table 1. Univariable analysis revealed the location of tumor, peritumoral bile duct dilatation, diffuse bile duct dilatation and proportion of the arterial enhancement to be significant parameters for differentiating between two groups (P = .004, <.0001, .048, .002, respectively). These significant factors are reported in Table 3 and figure 1.

Table 3. Comparison of gadoxetic acid-enhanced MR imaging features of intrahepatic mass-forming cholangiocarcinomas (ICCs) between patient with and without chronic liver disease (CLD) and statistically significant features from univariable analyses.

	CLD patients with ICC (n=20)	Non-CLD patients with ICC (n=45)	P value*
Location			.004†
Center	2(10)	21(46.7)	
Periphery	18(90)	24(53.3)	
Peritumoral bile duct dilatation			<.0001†
Yes	4(20)	32(71.1)	
No	16(80)	13(28.9)	
Diffuse bile duct dilatation			.048†
Yes	0(0)	9(20)	
No	20(100)	36(80)	
Proportion of arterial enhancement			.002†
>20% of the tumor area	11(55)	8(17.8)	
≤20% of the tumor area	9(45)	37(82.2)	

Note: Unless otherwise specified, values are numbers of patients and numbers

in parentheses are percentages. SI, signal intensity; Hyper/iso/hypoSI, relative to the liver parenchyma

*Chi-square test, or Fisher's exact test

†Statistically significant

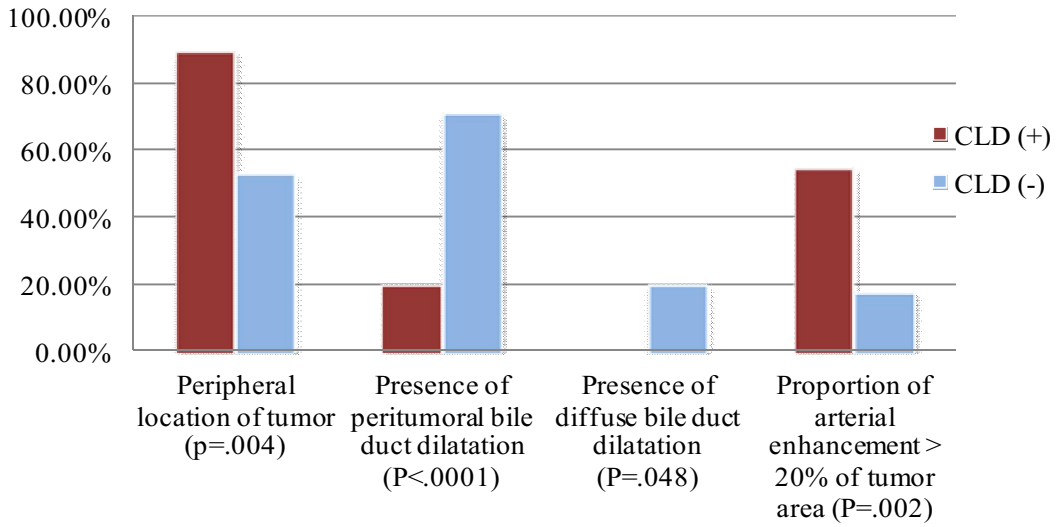

Figure 1. Statistically significant imaging features of univariable analyses. This graph shows more frequent peripheral location and larger proportion of arterial enhancement and less frequent peritumoral or diffuse bile duct dilatation of intrahepatic mass-forming cholangiocarcinoma (ICC) in patients with chronic liver disease (CLD) when compared to non-CLD patients.

The peripheral location of tumor was more commonly observed in group of CLD (90%, 18 of 20) than non-CLD group (53.3%, 24 of 45). The presence of peritumoral biliary dilatation was much lower in CLD patients (20%, 4 of 20) than non-CLD group (71.1%, 32 of 45) (Figure 2.).

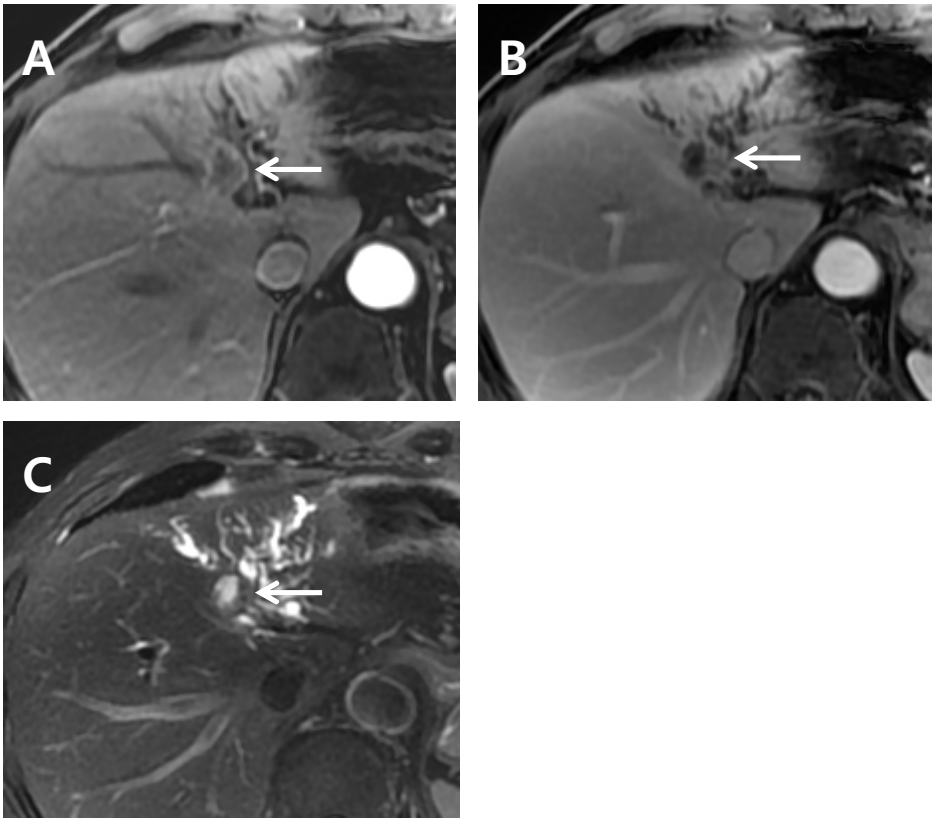

Figure 2. Surgically proven ICC without chronic liver disease in 75-year-old man. (A) On axial arterial phase image, about 1.7cm sized centrally located rim enhancing lobulated tumor is seen. This tumor was counted as less than 20% of arterial enhancement. (B) The tumor shows progressive enhancement on portal venous phase image. (C) The breath-hold T2 weighted image shows a prominent peritumoral bile duct dilatation. Not presented, but no target sign is seen on hepatobiliary phase image nor diffusion weighted image.

No diffuse bile duct dilatation was seen in CLD patients (0%, 0 of 20), but 9 cases of 45 (20%) showed diffuse bile duct dilatation in non-CLD patients. The arterial enhancement proportion of tumor larger than 20% of lesion was more frequently observed in CLD group (55%, 11 of 20) compared to non-CLD group (17.8%, 8 of 45) (Figure 3 and 4.).

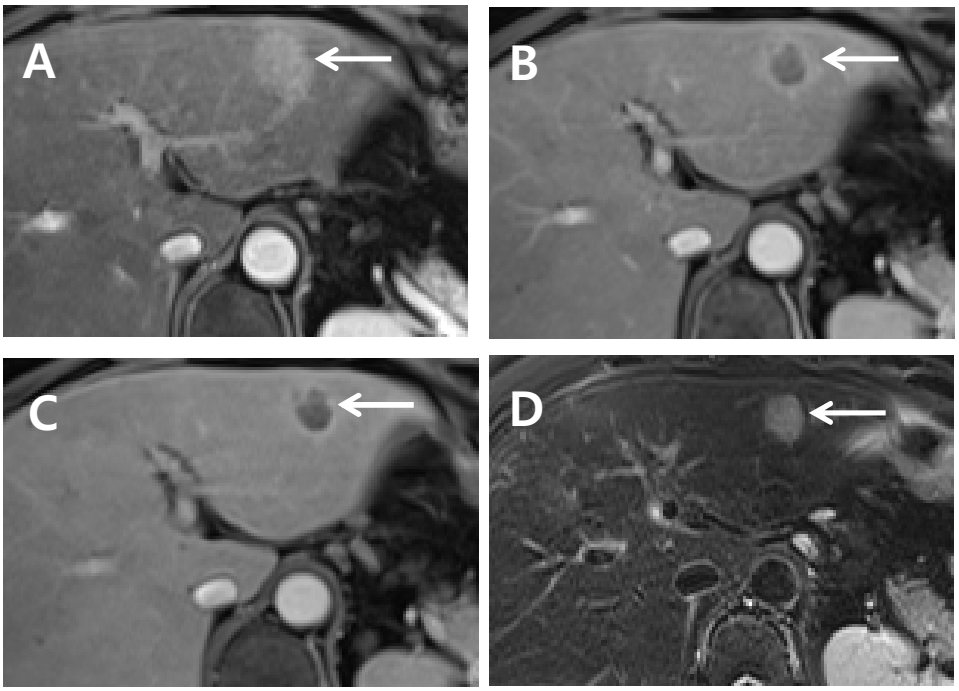

Figure 3. Surgically proven ICC with chronic liver disease in 58-year-old woman. (A) About 2cm sized peripheral located tumor in left lateral segment of the liver shows global arterial enhancement. (B) Wash-out pattern of enhancement is seen on portal phase image. (C) Rim-like enhancement is seen on late phase. (D) No peritumoral nor diffuse biliary dilatation is noted on T2-weighted image. Not presented, but no target sign is seen on hepatobiliary phase image nor diffusion weighted image.

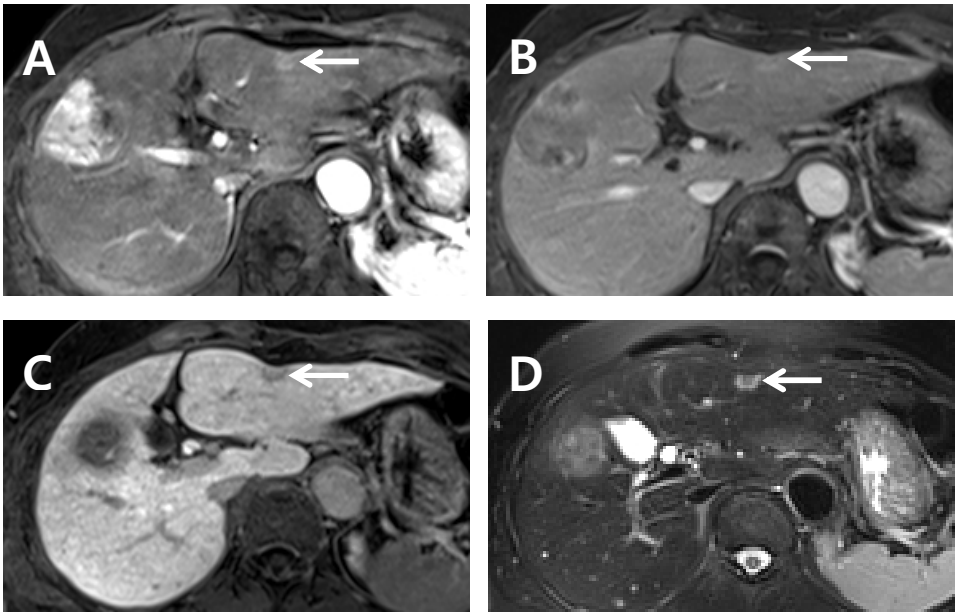

Figure 4. Surgically proven ICC with chronic liver disease in 65-year-old woman. About 4.5 cm sized hypervascular mass with internal necrosis and wash-out pattern of enhancement in right lobe of the liver. This mass was confirmed as HCC. In the left lobe, an about 1 cm sized peripheral located tumor with adjacent capsular retraction is seen. This tumor was confirmed as ICC. (A) The tumor shows global arterial enhancement, and (B) relatively stable dynamic enhance pattern. (C) Target sign is seen on hepatobiliary phase image. (D) No peritumoral or diffuse biliary dilatation is noted on T2-weighted image.

Results of multivariable logistic regression analysis identified that the no peritumoral bile duct dilatation (Odds ratio=5.589) and the proportion of arterial enhancement of tumor area larger than 20%(Odds ratio=4.719) was the significant and independent imaging features for the ICCs in the CLD patients compared relatively normal background liver patient (P = 0.028, 0.028, respectively) (Table 4.). The proportion of arterial enhancing, delayed wash-out enhancement pattern of the ICCs like HCC (Figure 3.) was relatively small (6.2%, 4 of 65, two were in CLD group and two were in non-CLD group).

Table 4. Multivariable analysis results from logistic regression analysis of significant variables associated with the differentiation of intrahepatic mass-forming cholangiocarcinomas (ICCs) in patient with chronic liver disease (CLD) from ones in patient without CLD.

	P value	Odds ratio	95 % Confidence interval of odds ratio	
Peripheral location	.303	2.717	.405	18.218
No peritumoral bile duct dilatation	.028†	5.589	1.202	25.984
No diffuse bile duct dilatation	.999		.000	
Proportion of arterial enhancement > 20%	.028†	4.719	1.184	18.814

Note: Odds ratio of no diffuse bile duct dilatation was omitted because of the extremely large value to be presented and statistical insignificance.

†Statistically significant

Analysis of arterial enhancement pattern and dynamic enhancement pattern which can resemble imaging features of HCC were also done. The proportion of wash-out enhancement pattern of the ICCs like HCC was relatively small (6.2%, 4 of 65, two were in CLD group and two were in non-CLD group). Most of ICCs presented rim-like arterial enhancement (70%, 14 of 20 in CLD group and 82.2%, 37 of 45 in non-CLD group), but minor portion of ICCs showed global enhancement (15%, 3 of 20 in CLD group and 4.4%, 2 of 45 in non-CLD group.

Overall inter-observer agreement was moderate degree (κ = 0.482). Inter-observer agreement of multiplicity and hypointense rim on T2-weighted image was almost perfect and tumor location, hepatic capsular retraction, peritumoral bile duct dilatation, diffuse bile duct dilatation and parenchymal atrophy were substantial. Most of imaging features presented moderate degree of inter-observer agreement, such as tumor margin, shape, satellite nodules, hepatolithiasis, portal vein encasement, hepatoduodenal lymphadenopathy, arterial enhancement pattern, arterial enhancement proportion of tumor larger than 20%, peritumoral enhancement, late phase signal intensity and hepatobiliary phase signal intensity. Fair degree of inter-observer agreement was seen in central necrosis, target sign on diffusion weighted image and target sign on hepatobiliary phase. Inter-observer agreement of texture of tumor, portal vein thrombosis, dynamic enhancement pattern and hyperintense rim on late phase were small and because of no positive results, no available result was obtained from imaging features of fat signal, mosaic pattern and nodule in nodule appearance.

No significant difference in recurrence free survival rate between two groups in the Kaplan-Meier curve and Log rank test (CLD group ; 47.4% vs. non-CLD group ; 16.5%), P=.298.

IV. DISCUSSION

According to our study, there were more frequent imaging features of ICC in CLD patients compared to non-CLD patients as follows: (1) peripheral location; (2) no peritumoral bile duct dilatation; (3) no diffuse bile duct dilatation; and (4) larger proportion of arterial enhancement. Among them, no peritumoral bile duct dilatation and larger area of arterial enhancement was the significant radiologic feature of ICC in CLD patients as compared to those without CLD on multivariate analysis. The fact that ICC in CLD patients has the large area of arterial enhancement of the tumor has important clinical meaning. Some ICCs arising from the CLD patients can mimic enhancement pattern of HCC due to large area of arterial enhancement, leading to misdiagnosis. Considering the increased incidence of ICC in patients with CLD, it is problematic to distinguish ICC from HCC [4,8,10]. Because usual HCC is not associated with bile duct dilatation, lack of peritumoral bile duct dilatation is of little importance in regard to differentiation of ICC from HCC in the CLD patients.

Typical enhancement patterns of mass-forming ICC on gadoxetic acid–enhanced MR images are thin peripheral rim and delayed heterogeneous enhancement during the dynamic phase [14]. The enhancement pattern of ICC correlates well with histopathology. The peripheral portion of ICC consists of abundant viable tumor cells and vessels while the central area of the ICC is composed of coagulative necrosis and scanty tumor cells. The fibrous stroma in the center of the tumor is known to show delayed enhancement on dynamic studies. Classically ICCs can be classified into mass-forming, periductal infiltrating, and intraductal growth types according to their gross morphologic features established by the Liver Cancer Study Group of Japan [15]. Recently some studies divided ICCs into two main forms on the basis of their origin, perihilar large bile duct type originating peribiliary glands and peripheral small

bile duct type arising from the canals of Hering [9,16,17]. Histologically the peripheral type ICC is grossly mass-forming type and shows higher density of tumor microvessels and arteries. According to the previous study, the arterial and microvessel density of ICC in the cirrhotic liver was higher than that in the liver of reactive change and correlated with increased arterial enhancement on CT and MRI using extracellular contrast agent [18]. The current study using gadoxetic acid-enhanced MR imaging is consistent with the histologic feature of the peripheral small duct type ICC and the previous study using extracellular contrast agent enhanced CT or MRI. Our univariable analysis identified that 55% (11 of 20) of the ICCs in CLD group showed more larger area of arterial enhancement, we believe that these large area of arterial enhancement in patients with CLD is attributed to increased microvessel densities in the tumors.

The increased enhancement on arterial phase images can be a confusing radiologic feature of ICC in the setting of CLD, misleading the observers to the diagnosis of HCC. Moreover, with the increased use of gadoxetic acid, dynamic enhancement patterns of ICC should be interpreted with caution. In contrast to extracellular agent, hepatic parenchyma shows gradually increased enhancement during transitional and hepatobiliary phase MR imaging when using gadoxetic acid as contrast agent. The hyperenhancement on arterial phase and washout during transitional phase and HBP are crucial to the invasive diagnosis of HCC as suggested by several guidelines. Therefore, to avoid misinterpretation of ICC as HCC, we need to interpret gadoxetic acid-enhanced MRI by combining both dynamic images and other sequences. Studies have shown that imaging features including lobulated shape, absence of fat, rim enhancement on arterial phase, target appearance on diffusion-weighted images and hepatobiliary phase on gadoxetic acid-enhanced MRI favor ICC over HCC. Hypointense rim on the HBP and heterogeneous signal intensity on T2 weighted image can be helpful when distinguishing ICC from HCC using

gadoxetic acid-enhanced MR imaging [19]. Recent study also revealed that ICC in cirrhotic liver shows rim-like or diffuse enhancement on arterial phase, followed by either a progressive or a sustained enhancement on the portal venous or transitional phases with enhancement defect on hepatobiliary phase [20]. Our study identified similar results. The majority of ICC in CLD group showed progressive enhancement on portal venous or transitional phase and only minor portion (10%, 2 of 20) of the ICC in CLD group showed wash-out pattern of enhancement. Furthermore, one tumor in the wash-out enhancement pattern in CLD group showed rim-like arterial enhancement with target sign on hepatobiliary phase and the other tumor presented global enhancement on arterial phase with rim-like enhancement on transitional phase. However, since there are still overlaps of imaging features between ICC and HCC with atypical enhancement pattern especially in CLD, clinical factors and pathologic confirmation through biopsy should also be considered.

In addition to the large area of arterial enhancement our result correlates with the histopathologic features of small duct type ICC. In our study, ICCs in CLD patients tends to have more peripheral location and less frequent peritumoral bile duct dilatation. It may be because the tumor involves peripherally located intrahepatic small bile ducts such as septal and interlobular bile ducts, connecting to the canals of Hering or bile ductules [9]. Considering common risk factors such as cirrhosis, HBC, HCV and metabolic syndrome, the molecular pathogenesis of peripheral small duct type ICC may have resemblance with that of HCC [8]. Thus peripheral small duct type ICC is less likely to be accompanied by ductal dilatation like HCC. However, the pathogenesis of perihilar large duct type ICC believed to be associated with chronic biliary inflammation. Chronic biliary inflammation may induce biliary intraepithelial neoplasia (BilIN) or periductal infiltration carcinoma. These type tumors progress with invasion to the liver parenchyma, then have the morphologic features of mass-forming and periductal infiltrating type tumor. Moreover,

intraductal spreading and desmoplasia of carcinoma in perihilar large duct type can lead to frequent ductal dilatation. We carefully suggest that ICC located in the periphery of the liver showing prominent arterial enhancement and not accompanied by ductal dilatation can be included in peripheral small duct type.

It has been suggested that there is a negative correlation between intratumoral arterial vessels and tumor progression of ICC. ICC having many arterial vessels may have well-preserved portal tracts accompanied by arterial vessels. As the tumor grows, engulfed portal tracts are destroyed. Therefore decreased intratumoral arteries indicate portal tract destruction and are related to aggressive tumor behavior [21]. Studies have shown that hypovascularity of ICCs correlates with higher histological malignancy such as perineural invasion [22] and patients with early enhancement in arterial phase tend to have significantly better survival than patients with hypovascular or ring enhancing tumor [23]. But in our study, because of insufficient enrolled number of patients, we could not obtain the significant difference in recurrence free survival rate between two groups, in spite of more arterial enhancing ICCs were included in CLD group. We also could not assess whether the outcomes of arterial enhancing ICCs are better than hypovascular tumor in CLD due to small sample size. Small duct type ICCs show a central fibrous area with dense carcinoma cells in the periphery of the tumor whereas large duct type ICCs have diffusely scattered fibrous stroma. The central fibrous stroma of small duct type ICCs is correlated with the delayed enhancement on dynamic CT scans or hepatobiliary phase MRI and could be a poor prognostic factor in mass-forming type ICCs [22,24]. Further study is required to evaluate whether the increased arterial enhancement and delayed enhancement on CT or MRI could be used as a prognostic imaging marker for ICCs.

Our study has several limitations. First, retrospective nature of our study may have selection bias. Second, since the sample size was small, we could not analyze the subgroups of CLD patients based on etiology or presence of

cirrhosis and there was a discrepancy between univariate and multivariate analysis. Third, we could not correlate imaging features with histopathology of ICC because histopathologic subclassification into small duct type ICC and large duct type ICC was not feasible in our institution.

V. CONCLUSION

In conclusion, ICCs arising in CLD patient show larger areas of arterial enhancement on gadoxetic acid-enhanced MR imaging and less peritumoral bile duct dilatation on T2-weighted MR image than those developed in non-CLD patient. We suggest that it is more helpful that future study regarding the comparison of imaging features of the HCC and ICC should be done in CLD patients to distinguish the arterial enhancing ICC from the HCC.

REFERENCES

1. Ros PR, Buck JL, Goodman ZD, Ros AM, Olmsted WW. Intrahe patic cholangiocarcinoma: radiologic-pathologic correlation. Radiolo gy 1988;167:689-93.
2. Patel T. Increasing incidence and mortality of primary intrahepatic cholangiocarcinoma in the United States. Hepatology 2001;33:135 3-7.
3. Malhi H, Gores GJ. Cholangiocarcinoma: modern advances in un derstanding a deadly old disease. J Hepatol 2006;45:856-67.
4. Singh P, Patel T. Advances in the diagnosis, evaluation and mana gement of cholangiocarcinoma. Curr Opin Gastroenterol 2006;22:2 94-9.
5. Endo I, Gonen M, Yopp AC, Dalal KM, Zhou Q, Klimstra D, et al. Intrahepatic cholangiocarcinoma: rising frequency, improved s

urvival, and determinants of outcome after resection. Ann Surg 2008;248:84-96.

6. Tyson GL, El-Serag HB. Risk factors for cholangiocarcinoma. Hepatology 2011;54:173-84.
7. Shin HR, Oh JK, Masuyer E, Curado MP, Bouvard V, Fang YY, et al. Epidemiology of cholangiocarcinoma: an update focusing on risk factors. Cancer Sci 2010;101:579-85.
8. Palmer WC, Patel T. Are common factors involved in the pathogenesis of primary liver cancers? A meta-analysis of risk factors for intrahepatic cholangiocarcinoma. J Hepatol 2012;57:69-76.
9. Aishima S, Oda Y. Pathogenesis and classification of intrahepatic cholangiocarcinoma: different characters of perihilar large duct type versus peripheral small duct type. J Hepatobiliary Pancreat Sci 2015;22:94-100.
10. Forner A, Llovet JM, Bruix J. Hepatocellular carcinoma. Lancet 2012;379:1245-55.
11. DeOliveira ML. Liver transplantation for cholangiocarcinoma: current best practice. Curr Opin Organ Transplant 2014;19:245-52.
12. Hammerstingl R, Huppertz A, Breuer J, Balzer T, Blakeborough A, Carter R, et al. Diagnostic efficacy of gadoxetic acid (Primovist)-enhanced MRI and spiral CT for a therapeutic strategy: comparison with intraoperative and histopathologic findings in focal liver lesions. Eur Radiol 2008;18:457-67.
13. Kundel HL, Polansky M. Measurement of Observer Agreement 1. Radiology 2003;228:303-8.
14. Kang Y, Lee JM, Kim SH, Han JK, Choi BI. Intrahepatic mass-forming cholangiocarcinoma: enhancement patterns on gadoxetic acid-enhanced MR images. Radiology 2012;264:751-60.
15. Japan LCSGo. Classification of primary liver cancer. Tokyo: Kane

hara 1997;1:997.

16. Cardinale V, Carpino G, Reid L, Gaudio E, Alvaro D. Multiple c ells of origin in cholangiocarcinoma underlie biological, epidemiol ogical and clinical heterogeneity. World J Gastrointest Oncol 201 2;4:94-102.
17. Aishima S, Kuroda Y, Nishihara Y, Iguchi T, Taguchi K, Taketo mi A, et al. Proposal of progression model for intrahepatic chola ngiocarcinoma: clinicopathologic differences between hilar type an d peripheral type. Am J Surg Pathol 2007;31:1059-67.
18. Xu J, Igarashi S, Sasaki M, Matsubara T, Yoneda N, Kozaka K, et al. Intrahepatic cholangiocarcinomas in cirrhosis are hypervascu lar in comparison with those in normal livers. Liver Int 2012;32: 1156-64.
19. Kim R, Lee JM, Shin CI, Lee ES, Yoon JH, Joo I, et al. Differ entiation of intrahepatic mass-forming cholangiocarcinoma from he patocellular carcinoma on gadoxetic acid-enhanced liver MR imag ing. Eur Radiol 2015; doi:10.1007/s00330-015-4005-8.
20. Piscaglia F, Iavarone M, Galassi M, Vavassori S, Renzulli M, For zenigo LV, et al. Cholangiocarcinoma in Cirrhosis: Value of Hepa tocyte Specific Magnetic Resonance Imaging. Dig Dis 2015;33:73 5-44.
21. Aishima S, Iguchi T, Nishihara Y, Fujita N, Taguchi K, Taketomi A, et al. Decreased intratumoral arteries reflect portal tract destr uction and aggressive characteristics in intrahepatic cholangiocarci noma. Histopathology 2009;54:452-61.
22. Asayama Y, Yoshimitsu K, Irie H, Tajima T, Nishie A, Hirakawa M, et al. Delayed-phase dynamic CT enhancement as a prognost ic factor for mass-forming intrahepatic cholangiocarcinoma. Radiol ogy 2006;238:150-5.

23. Nanashima A, Sumida Y, Abo T, Oikawa M, Murakami G, Takes hita H, et al. Relationship between pattern of tumor enhancement and clinicopathologic characteristics in intrahepatic cholangiocarci noma. J Surg Oncol 2008;98:535-9.

24. Koh J, Chung YE, Nahm JH, Kim HY, Kim KS, Park YN, et al. Intrahepatic mass-forming cholangiocarcinoma: prognostic value o f preoperative gadoxetic acid-enhanced MRI. Eur Radiol 2015; do i:10.1007/s00330-015-3846-5.

APPENDICES

Table 1. Comparison of gadoxetic acid-enhanced MR imaging features of intrahepatic mass-forming cholangiocarcinomas (ICCs) between patient with and without chronic liver disease (CLD) and univariable analyses results

	CLD patients with ICC (n=20)	Non-CLD patients with ICC (n=45)	P value*
Location			.004†
Center	2(10)	21(46.7)	
Periphery	18(90)	24(53.3)	
Margin			.340
Smooth	11(55)	19(42.2)	
Irregular	9(45)	26(74.3)	
Contour			.262
Round	5(25)	5(11.1)	
Lobulated	15(75)	40 (88.9)	
Texture			1.000
Homogeneous	3(15)	6(13.3)	
Heterogeneous	17(85)	39(86.7)	
Presence of central necrosis			.791
Yes	14(70)	30(66.7)	
No	6(30)	15(33.3)	
Presence of satellite nodule (located < 2cm from the tumor)			.079
Yes	6(30)	5(11.1)	
No	14(70)	40(88.9)	
Multifocality (located >2cm apart from the tumor),			.057
Yes	6(30)	4(8.9)	
No	14(70)	41(91.1)	
Adjacent liver capsule retraction			.495
Yes	7(35)	12(26.7)	
No	13(65)	33(73.3)	
Peritumoral bile duct dilatation			<.0001†

Yes	4(20)	32(71.1)	
No	16(80)	13(28.9)	
Diffuse bile duct dilatation			.048†
Yes	0(0)	9(20)	
No	20(100)	36(80)	
Hepatolithiasis,			.303
Yes	0(0)	4(8.9)	
No	20(100)	41(91.1)	
Parenchymal atrophy			.725
Yes	4(20)	7(15.6)	
No	16(80)	38(84.4)	
Portal vein encasement/obliteration			.315
Yes	5(25)	17(37.8)	
No	15(75)	28(62.2)	
Portal vein thrombosis			.091
Yes	2(10)	0(0)	
No	18(90)	45(100)	
Hepatoduodenal lymphadenopathy (short axis diameter >1cm)			.184
Yes	5(25)	19(42.2)	
No	15(75)	26(57.8)	
Pattern of arterial enhancement			.310
Rim-like	14(70)	37(82.2)	
Global	3(15)	2(4.4)	
Mixed/irregular	3(15)	6(13.3)	
Proportion of arterial enhancement			.002†
>20% of the tumor area	11(55)	8(17.8)	
≤20% of the tumor area	9(45)	37(82.2)	
Dynamic enhancement pattern			.660
Progressive	16(80)	38(84.4)	
Stable	2(10)	5(11.1)	
Wash-out	2(10)	2(4.4)	
Peritumoral hyperemia			.747
Yes	15(75)	36(80)	
No	5(25)	9(20)	

Signal on late phase			.368
LowSI	18(90)	42(93.3)	
IsoSI	1(5)	3(6.7)	
HyperSI	1(5)	0(0)	
Hyperintense rim on late phase			1.000
Yes	5(25)	11(24.4)	
No	15(75)	34(75.6)	
Hypointense rim on T2-weighted image			.547
Yes	0(0)	3(6.7)	
No	20(100)	42(93.3)	
Target appearance on high b-value diffusion-weighted image (hypointensity with peripheral hyperintense rim)			.262
Yes	11(55)	18(60)	
No	9(45)	27(40)	
Signal on hepatobiliary phase,			1.000
HyperSI	0(0)	0(0)	
IsoSI	0(0)	1(2.2)	
LowSI	20(100)	44(97.8)	
Target appearance on hepatobiliary phase (central enhancement with hypointense rim).			.208
Yes	14(70)	24(53.3)	
No	6(30)	21(46.7)	

Note: Unless otherwise specified, values are numbers of patients and numbers in parentheses are percentages. SI, signal intensity; Hyper/iso/hypoSI, relative to the liver parenchyma

*Chi-square test, or Fisher's exact test

†Statistically significant

ABSTRACT(IN KOREAN)

만성 간질환 환자와 비질환자에서 종괴 형성형 간내담관암의 Gadoxetic acid 조영 증강 자기공명영상 소견의 차이

<지도교수 김명진>

연세대학교 대학원 의학과
김재민

목적: 비질환자와 비교하였을 때 만성 간질환 환자에서 발생하는 종괴 형성형 간내담관암의 Gadoxetic acid 조영제를 사용한 자기공명영상 소견의 차이를 확인하기 위함.

방법: 후향적 설계로 간 절제술로 진단된 총 65명의 종괴 형성형 간내담관암 환자 중 20명은 만성 간질환 환자로 확인되었으며, 45명은 비질환자로 분류됨. 두 군에서 다양한 Gadoxetic acid 조영 증강 자기공명영상 소견을 비교하였으며, 통계적으로 유의미한 단변량 분석 결과에 대하여서는 다변량 분석을 시행함.

결과: 단변량 분석에서 만성 간질환 환자에서 발생하는 종괴 형성형 간내담관암은 비질환자에 비해 더 원위부에 위치하였으며, 동맥기 조영 증강이 20%를 초과하는 경우가 더 많았으나 종괴 주위 및 전반적인 담관 확장을 동반하는 경우는 더 적었음. 이 네 가지 소견의 다변량 분석 결과 동맥기 조영증강이 종괴 면적의 20%를 초과하는 경우 (P = .028, B = 1.552, odds ratio = 4.719) 및 종괴 주위 담관 확장이 없는 경우 (P = .028, B = 1.721, odds ratio = 5.589) 가 만성 간질환 환자의 종괴 형성형 간내담관암을 유의미하게 시사하는 소견이었음.

결론: 만성 간질환 환자에서 발생하는 종괴 형성형 간내담관암은 비간질환 환자에 비해 Gadoxetic acid 조영 증강 자기공명영상에서 동맥기에 더 넓은 영역에서 조영 증강을 보이며 T2 강조영상에서 종괴 주위 담관 확장이 없는 소견을 보임.

핵심되는 말: 담관암, 진단, 만성 간질환, 자기공명영상, Gadoxetic acid